The Astrophysical Journal, 823:158 (8pp), 2016 June 1 doi:10.3847/0004-637X/823/2/158

THE EFFECT OF ^{22}Ne DIFFUSION IN THE EVOLUTION AND PULSATIONAL PROPERTIES OF WHITE DWARFS WITH SOLAR METALLICITY PROGENITORS

María E. Camisassa[1,2], Leandro G. Althaus[1,2], Alejandro H. Córsico[1,2], Núria Vinyoles[3,4], Aldo M. Serenelli[3,4], Jordi Isern[3,4], Marcelo M. Miller Bertolami[2,5], and Enrique García–Berro[4,6]

[1] Facultad de Ciencias Astronómicas y Geofísicas, Universidad Nacional de La Plata, Paseo del Bosque s/n, 1900 La Plata, Argentina; camisassa@fcaglp.unlp.edu.ar
[2] Instituto de Astrofísica de La Plata, UNLP-CONICET, Paseo del Bosque s/n, 1900 La Plata, Argentina
[3] Instituto de Ciencias del Espacio (CSIC), Carrer de Can Magrans s/n, E-08193, Cerdanyola del Vallés, Spain
[4] Institute for Space Studies of Catalonia, c/Gran Capità 2-4, Edif. Nexus 201, E-08034 Barcelona, Spain
[5] Max-Planck-Institut für Astrophysik, Karl-Schwarzschild-Strasse 1, D-85748, Garching, Germany
[6] Departament de Física, Universitat Politècnica de Catalunya, c/Esteve Terrades 5,E-08860 Castelldefels, Spain
Received 2016 February 3; accepted 2016 March 22; published 2016 June 1

ABSTRACT

Because of the large neutron excess of ^{22}Ne, sedimentation of this isotope occurs rapidly in the interior of white dwarfs. This process releases an additional amount of energy, thus delaying the cooling times of the white dwarf. This influences the ages of different stellar populations derived using white dwarf cosmochronology. Furthermore, the overabundance of ^{22}Ne in the inner regions of the star modifies the Brunt–Väisälä frequency, thus altering the pulsational properties of these stars. In this work we discuss the impact of ^{22}Ne sedimentation in white dwarfs resulting from solar metallicity progenitors ($Z = 0.02$). We performed evolutionary calculations of white dwarfs with masses of 0.528, 0.576, 0.657, and 0.833 $M_{\odot}$ derived from full evolutionary computations of their progenitor stars, starting at the zero-age main sequence all the way through the central hydrogen and helium burning, the thermally pulsing asymptotic giant branch (AGB), and post-AGB phases. Our computations show that at low luminosities ($\log(L/L_{\odot}) \lesssim -4.25$), ^{22}Ne sedimentation delays the cooling of white dwarfs with solar metallicity progenitors by about 1 Gyr. Additionally, we studied the consequences of ^{22}Ne sedimentation on the pulsational properties of ZZ Ceti white dwarfs. We find that ^{22}Ne sedimentation induces differences in the periods of these stars larger than the present observational uncertainties, particularly in more massive white dwarfs.

Key words: asteroseismology – dense matter – diffusion – stars: evolution – stars: interiors – white dwarfs

1. INTRODUCTION

White dwarf stars are the most common end point of stellar evolution. They provide a wealth of information about the evolution of their progenitor stars and the physical processes occurring in stars. They also provide valuable information about the star formation history of the solar neighborhood and allow us to study the properties of various stellar populations (see Fontaine & Brassard 2008, Winget & Kepler 2008, and Althaus et al. 2010b for reviews). In particular, white dwarfs are used as accurate age indicators for a wide variety of Galactic populations, including the disk and open and globular clusters (see Winget et al. 2009, García-Berro et al. 2010, Jeffery et al. 2011, Bono et al. 2013, Hansen et al. 2013, and Torres et al. 2015 for some recent applications).

The use of white dwarfs as reliable and precise clocks to date stellar populations has prompted the computation of detailed and complete evolutionary models for these stars, taking into account all of the relevant sources and sinks of energy and the evolutionary history of progenitor stars (Renedo et al. 2010; Salaris et al. 2010; Althaus et al. 2012, 2015). The computation of such models requires a detailed knowledge of the main physical processes responsible for their evolution. Among these processes relevant to the present paper, is the slow gravitational settling of ^{22}Ne in the liquid phase, which has been shown to strongly decrease the cooling rate of white dwarfs resulting from high-metallicity ($Z \gtrsim 0.03$) progenitors (García-Berro et al. 2008; Althaus et al. 2010c). ^{22}Ne is the most abundant impurity present in the carbon–oxygen interiors of typical white dwarfs and is the result of helium burning of the ^{14}N built up during the CNO cycle. In particular, the two additional neutrons present in the ^{22}Ne nucleus (relative to $A = 2Z$) result in a net downward gravitational force and a slow settling of ^{22}Ne in the liquid regions toward the center of the white dwarf (Bravo et al. 1992). The role of ^{22}Ne sedimentation in the energetics of crystallizing white dwarfs was first addressed by Isern et al. (1991) and quantitatively explored later by Deloye & Bildsten (2002) and Althaus et al. (2010c). These studies showed that ^{22}Ne sedimentation releases substantial energy to appreciably modify the cooling of massive white dwarfs, delaying the evolution by about 10^9 years at low luminosities ($\log L/L_{\odot} \lesssim -4.5$). The occurrence of this process in the interior of cool white dwarfs has been shown to be a key factor in solving the long-standing age discrepancy of the metal-rich cluster NGC 6791 (García-Berro et al. 2010).

The studies of García-Berro et al. (2008) and Althaus et al. (2010c) revealed the necessity of including the gravitational energy released by ^{22}Ne sedimentation in the calculations of detailed white dwarf cooling sequences. Motivated by these findings, in this paper we investigate the impact of ^{22}Ne sedimentation on the cooling age of white dwarfs resulting from solar metallicity progenitors. Our aim is to provide an accurate assessment of the differences in the cooling ages when this process is neglected. The results presented here improve our previous works in two ways. First, the calculations presented here include realistic initial ^{22}Ne abundance distributions in the white dwarf interior, resulting from the evolutionary history of progenitor stars. In particular, we compute the full evolution of progenitor stars starting from the zero-age main sequence (ZAMS) all the way through the phases of hydrogen and helium core burning and the thermally

Table 1
Basic Model Properties for Our Sequences

M_{ZAMS} ($M_\odot$)	M_{WD} ($M_\odot$)	$t_{pre\text{-}WD}$ (Gyr)	C/O
1.0	0.528	11.813	0.3009
1.5	0.576	2.820	1.6488
3.0	0.657	0.443	1.1434
4.0	0.833	0.196	4.0894

Note. We List the Mass at the zero-age main sequence (M_{ZAMS}); the mass of the resulting white dwarf (M_{WD}); the age at the beginning of white dwarf cooling sequence, defined at the moment when the star reaches the maximum effective temperature, $t_{pre\text{-}WD}$; and the surface carbon-to-oxygen ratio at the beginning of the white dwarf stage (C/O).

pulsing asymptotic giant branch (AGB). In this way we obtained realistic initial ^{22}Ne profiles at the beginning of the white dwarf cooling sequence, which is necessary to accurately compute the energy released by the slow ^{22}Ne sedimentation along the entire white dwarf cooling track. Second, the physical description of ^{22}Ne diffusion in strongly coupled plasma mixtures is substantially improved. Specifically, in our calculations we employ the new diffusion coefficients for ^{22}Ne based on the molecular dynamics simulations of ^{12}C, ^{16}O, and ^{22}Ne mixtures of Hughto et al. (2010). These diffusion coefficients are now accurately known. Thus, the remaining uncertainties in their specific values should not be relevant for white dwarf evolutionary calculations.

We extend the scope of the paper by exploring the consequences of ^{22}Ne sedimentation for the adiabatic pulsational properties of ZZ Ceti stars. To this end, we perform an adiabatic, nonradial pulsation analysis of g-modes. The results presented here are the first ones in showing the impact of ^{22}Ne sedimentation on the expected spectrum of pulsation periods of evolving ZZ Ceti star models.

2. NUMERICAL SETUP AND INPUT PHYSICS

The evolutionary calculations discussed in this paper were done with an updated version of the LPCODE stellar evolutionary code (see Althaus et al. (2005) and references therein). This is a well-tested and calibrated code that has been amply used in the study of different aspects of the evolution of low-mass stars. Particularly, it has been used to compute very accurate and realistic white dwarf models (Miller Bertolami et al. 2008, 2011; Althaus et al. 2010a, 2013, 2015; García-Berro et al. 2010; Renedo et al. 2010; Wachlin et al. 2011; Córsico et al. 2012). A recent test comparing LPCODE with a different white dwarf evolutionary code shows that uncertainties in the white dwarf cooling ages that result from the different numerical implementations of the stellar evolution equations are less than 2% (Salaris et al. 2013). A detailed description of the input physics and numerical procedures can be found in these works. In this section we briefly summarize the main input physics for this work.

In this work initial white dwarf models have been derived from the full evolutionary history of their progenitor stars, including the central hydrogen and helium burning, the thermally pulsing AGB, and the post-AGB. The initial metallicity of the sequences has been set to $Z = 0.02$. The initial masses of our sequences and the resulting white dwarf masses are listed in Table 1 together with the pre-white dwarf age and the carbon-to-oxygen ratio at the beginning of the white dwarf stage before gravitational settling modifies it. The evolution of the models before the white dwarf stage is described in detail in Miller Bertolami (2015), to which the reader is referred.

In contrast with our previous studies of the impact of ^{22}Ne sedimentation on white dwarf evolution, in this work we have considered realistic initial ^{22}Ne profiles at the beginning of the cooling track. Relevant to this aspect, we mention that LPCODE considers a simultaneous treatment of non-instantaneous mixing (and extra-mixing if present), element diffusion (chemical and thermal diffusion plus gravitational settling), and nuclear burning of elements. The code treats convective boundary mixing as a diffusion process by assuming that mixing velocities decay exponentially beyond each convective boundary (Freytag et al. 1996; Herwig et al. 1997). Specifically, we assumed a diffusion coefficient $D_{OV} = D_O \exp(-2z/fH_p)$, where H_p is the pressure scale height at the convective boundary, D_O is the diffusion coefficient of unstable regions close to the convective boundary, and z is the geometric distance from the edge of the convective boundary. Convective boundary mixing has been considered during the core hydrogen- and helium-burning phases and in the thermally pulsing AGB. The convective boundary mixing efficiency f has been calibrated to different values in different convective boundaries to reproduce different observables during the pre-white dwarf phase (see Miller Bertolami (2015) for details). Radiative and conductive opacities are taken from the OPAL database (Iglesias & Rogers 1996) and from Cassisi et al. (2007), respectively. For the low-temperature regime we used the molecular opacities with varying carbon-to-oxygen ratios of Ferguson et al. (2005), presented in Weiss & Ferguson (2009). These opacities are necessary for a realistic treatment of the evolution of the progenitor during the thermally pulsing AGB phase. At low effective temperatures in the white dwarf regime, outer boundary conditions for the evolving models are derived from non-gray model atmospheres (Rohrmann et al. 2012). Latent heat and phase separation of carbon and oxygen due to crystallization have been included as energy sources, using the phase diagram of Horowitz et al. (2010).

Another improvement with respect to our previous studies is that we have included in this work the most recent determination of the ^{22}Ne diffusion coefficients (Hughto et al. 2010). We have also improved our numerical treatment for ^{22}Ne sedimentation by assuming that ^{22}Ne diffuses in a one-component plasma background consisting of a fictitious element with atomic weight (A) and atomic number (Z). In contrast with our previous treatment, here A and Z of the fictitious element are defined by the average A and Z in each layer and not assumed constant through different layers. Finally, the energy released by ^{22}Ne sedimentation as well as from crystallization is included locally in the equation of luminosity, following García-Berro et al. (2008) and Althaus et al. (2010c). The calculations presented here constitute the first grid of solar metallicity white dwarf evolutionary sequences that include the effects of ^{22}Ne sedimentation in a consistent way. Finally, for the sake of comparison, we have also performed additional evolutionary calculations in which ^{22}Ne sedimentation has been suppressed.

To improve upon previous works we also analyze the impact of ^{22}Ne sedimentation in the predicted pulsational spectrum of ZZ Ceti stars. For this, we employ the adiabatic version of the

LP-PUL pulsation code described in detail in Córsico & Althaus (2006), which is coupled to the LPCODE evolutionary code. The LP-PUL pulsation code is based on a general Newton–Raphson technique that solves the full fourth-order set of real equations and boundary conditions governing linear, adiabatic, nonradial pulsations following the dimensionless formulation of Dziembowski (1971; see Unno et al. 1989). The prescription we follow to assess the run of the Brunt–Väisälä frequency (N) for a degenerate environment typical of the deep interior of a white dwarf is the so-called "Ledoux Modified" treatment (Tassoul et al. 1990):

$$N^2 = \frac{g^2\rho}{P}\frac{\chi_{\rm T}}{\chi_\rho}[\nabla_{\rm ad} - \nabla + B], \quad (1)$$

where the compressibilities are defined as

$$\chi_\rho = \left(\frac{\partial \ln P}{\partial \ln \rho}\right)_{{\rm T},\{X_i\}} \quad \chi_{\rm T} = \left(\frac{\partial \ln P}{\partial \ln T}\right)_{\rho,\{X_i\}}. \quad (2)$$

The Ledoux term B is computed as (Tassoul et al. 1990):

$$B = -\frac{1}{\chi_{\rm T}}\sum_1^{M-1}\chi_{X_{\rm i}}\frac{d\ln X_i}{d\ln P}, \quad (3)$$

where

$$\chi_{X_{\rm i}} = \left(\frac{\partial \ln P}{\partial \ln X_i}\right)_{\rho,{\rm T},\{X_{\rm j\neq i}\}}. \quad (4)$$

3. RESULTS

3.1. Impact On White Dwarf Evolution

The inner chemical abundance distribution in terms of the outer mass fraction at the beginning of the cooling track of our 0.657 $M_\odot$ white dwarf sequence is shown in the upper panel of Figure 1. This figure shows the chemical stratification as given by the evolutionary history of the progenitor star. In particular, the ^{22}Ne abundance by mass is about 0.02 throughout the innermost region of the white dwarf. This abundance was mostly built up during the helium core burning phase and results from helium burning on ^{14}N via the reactions $^{14}{\rm N}(\alpha,\gamma)^{18}{\rm F}(\beta^+)^{18}{\rm O}(\alpha,\gamma)^{22}{\rm Ne}$. It is also worth noting the abrupt change of ^{22}Ne abundance at $\log(1-m_r/M_\star)\sim -2.5$, just below the pure helium buffer. This abrupt change in all chemical abundances shown in the figure marks the extent reached by the pulse-driven convection zone during the last thermal pulse on the AGB experienced by the progenitor star.

The bottom panel of Figure 1 shows the corresponding chemical stratification at the end of the cooling track when the surface luminosity is $\log(L/L_\odot) = -4.75$. Note that element diffusion has markedly changed the initial chemical abundance distribution. In particular, chemical transitions have been smoothed out by the diffusion processes. Note also that element diffusion has depleted ^{22}Ne in the outer regions of the core and enhanced it in the central region of the white dwarf. This takes place during those stages of the evolution during which the white dwarf core is liquid, and is more relevant for massive white dwarfs, owing to their larger gravities.

Deloye & Bildsten (2002), García-Berro et al. (2008), and Althaus et al. (2010c) have convincingly shown that the slow ^{22}Ne sedimentation process releases enough energy to strongly alter the evolution of white dwarfs characterized by a high

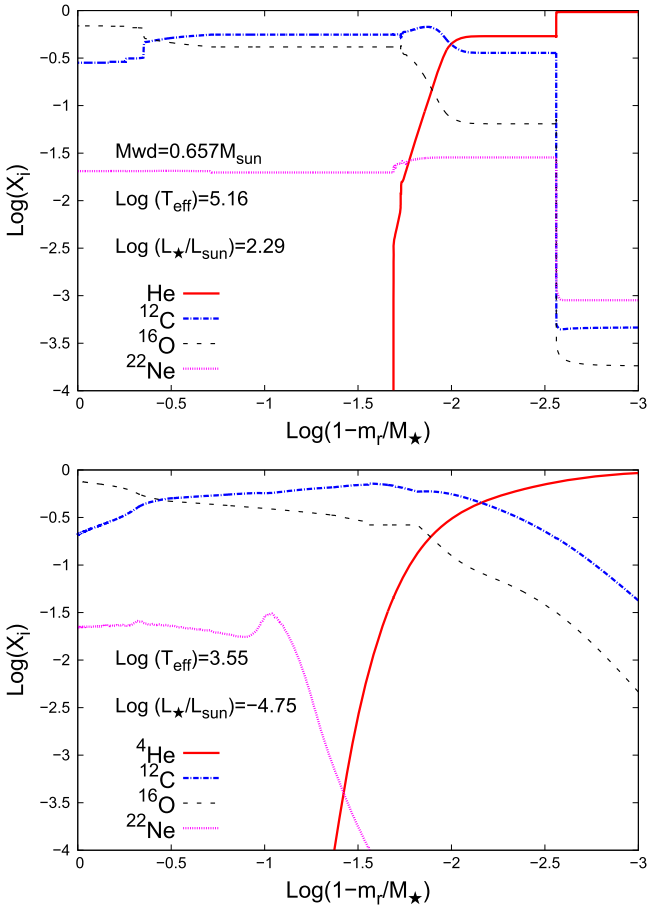

Figure 1. Logarithmic mass fractions of the elements in the 0.657 $M_\odot$ white dwarf model. The top panel shows the abundances at the beginning of the white dwarf cooling sequences, while the bottom panel shows the final abundances.

metal content in their interiors. Here we find that cooling times are substantially modified in the case of white dwarfs with solar metallicity progenitors. This can be inferred from Figure 2, which shows the white dwarf surface luminosity as a function of age for all our sequences. The solid red lines show the prediction when ^{22}Ne sedimentation is considered and the dotted lines show the prediction when ^{22}Ne sedimentation is suppressed. Time delays are shown in the right-hand panels. Note the substantial lengthening of the evolutionary times at low luminosities. At the luminosities typical of the cut-off of the white dwarf luminosity function, $\log(L/L_\odot)\approx -4.5$, time delays range from 0.7 to 1.2 Gyr, depending on the stellar mass (see Table 2). It should be mentioned that the oldest white dwarfs in the Galactic disk are likely low metallicity, so the impact of ^{22} Ne sedimentation on those white dwarfs should be less relevant. Also note that massive white dwarfs have larger gravities, therefore ^{22}Ne sedimentation is more effective. At low luminosities when the white dwarf crystallizes, ^{22}Ne stops diffusing inwards through the solid phase, therefore the time delay stops growing. This is reflected in the curve of the right-hand panels, as it becomes constant after crystallization. Time delays are slightly shorter in the 0.833 $M_\odot$ white dwarf model than in the 0.657 $M_\odot$ model because more massive white dwarfs crystallize at a higher luminosity, preventing ^{22}Ne to keep diffusing. In summary, ^{22}Ne sedimentation, a process not considered in most existing grids of white dwarf evolutionary sequences used to date stellar populations, induces substantial

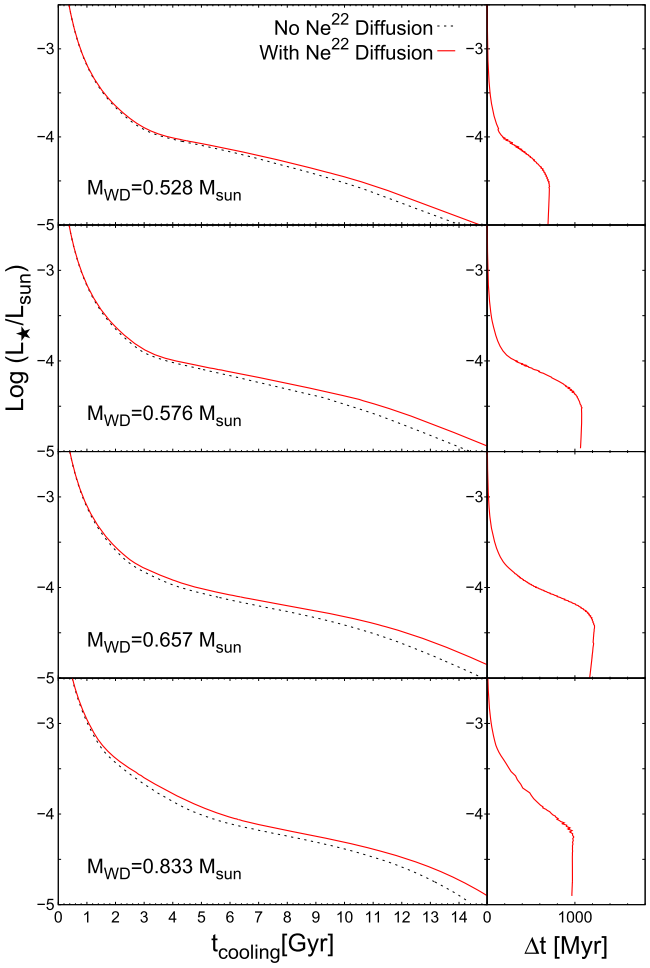

Figure 2. Impact of ^{22}Ne sedimentation on the cooling times, defined as the time since the star reaches its maximum effective temperature, for our four sequences. The dashed line shows the evolution when ^{22}Ne sedimentation is disregarded, while the solid red line shows the evolution for the white dwarf when ^{22}Ne sedimentation is included. Time delays in Myr are also shown in the right panels.

Table 2
White Dwarf Cooling Ages for Sequences with ^{22}Ne Diffusion and Their Corresponding Time Delays Compared with the Sequences in Which this Process is Disregarded

$-\log(L/L_{\odot})$	$t_{\rm cool}$ (Gyr)			
	0.528 $M_{\odot}$	0.576 $M_{\odot}$	0.657 $M_{\odot}$	0.833 $M_{\odot}$
1.0	0.02	0.02	0.01	0.01
2.0	0.16	0.16	0.17	0.21
3.0	0.77	0.80	0.86	1.06
4.0	3.92	4.15	4.83	5.65
4.5	10.45	11.33	12.10	12.13
5.0	14.68	15.29	16.01	15.52
	δt (Gyr)			
3.0	0.006	0.009	0.015	0.046
4.0	0.18	0.34	0.56	0.74
4.5	0.69	1.07	1.22	0.97

delays in the cooling times of white dwarfs with solar metallicity progenitors. Moreover, the lengthening of the cooling times is much longer than the uncertainties arising from current uncertainties in the microphysics and numerical inputs (Salaris et al. 2013). A more detailed comparison between model cooling sequences and the observed white dwarf luminosity function is thus desirable. We defer these comparisons to future work.

3.2. Asteroseismological Consequences

Early estimates of the impact of ^{22}Ne diffusion on the pulsation properties of ZZ Ceti stars was done by Deloye & Bildsten (2002), who found that this process could change the period of the high radial order g-modes by about 1%. In this section we perform a detailed analysis to provide a reliable assessment of the adiabatic pulsation properties of our white dwarf evolutionary models that take into account ^{22}Ne diffusion. We compute pulsation periods in the range $100 \lesssim \Pi \lesssim 3500$ s corresponding to dipole ($\ell = 1$) g-modes. Quantities relevant for the pulsational properties of our models are shown in Figure 3 for a selected 0.576 $M_{\odot}$ white dwarf model at $\log(T_{\rm eff}) = 4.01$. For comparison purposes, we show in the upper panel the chemical stratification of the model. Note that at this stage of the evolution, which corresponds to the domain of ZZ Ceti stars, element diffusion has markedly altered the initial ^{22}Ne distribution in the star. In particular, it has strongly smoothed out the abrupt change of the ^{22}Ne abundance at $\log(1 - m_r/M_{\star}) \sim -2.6$ and it has produced a bump in its abundance at $\log(1 - m_r/M_{\star}) \sim -1.5$. This bump is located at the tail of the helium distribution, where the average values of Z and A grow inwards, leading to a change in the diffusion coefficients at those layers. In particular, the diffusion coefficients decrease inwards at that interface, thus ^{22}Ne ions tend to accumulate. As the white dwarf evolves, this bump diffuses inward.

In the middle and bottom panels of Figure 3 we plot the run of the Ledoux term B and the logarithm of the squared Brunt–Väisälä frequency, respectively, for the same white dwarf model. We show the model including Ne^{22} sedimentation using solid lines, while dotted lines are employed for the model for which Ne^{22} sedimentation was neglected. As can be seen, ^{22}Ne sedimentation barely affects the shape of the Brunt–Väisälä frequency, being almost unnoticeable in the plot.

Because of the two additional neutrons of the ^{22}Ne nucleus (relative to $A = 2\,Z$ nuclei), changes in the ^{22}Ne abundance directly translate into appreciable changes in the pressure of the degenerate electron gas. By the time evolution has proceeded to the domain of the ZZ Ceti stars, ^{22}Ne has diffused toward the central regions of the star, so the outer layers of the core have already been depleted of this element. This behavior turns out to be markedly more noticeable for larger gravities. This can be seen in the upper panel of Figure 4, which shows the chemical abundance distribution of a selected 0.833 $M_{\odot}$ white dwarf model at $\log(T_{\rm eff}) = 4.04$. The consequences for the Ledoux term and the Brunt–Väisälä frequency can be inferred from the middle and bottom panels, respectively. Note in particular that the overabundance of ^{22}Ne in the inner regions of the star leads to an increase of the density and therefore to a global increase in the Brunt–Väisälä frequency in those regions.

The precise shape of the Brunt–Väisälä frequency largely determines the structure of the g-mode period spectrum. Because this quantity is modified by the overabundance of the ^{22}Ne in the inner regions of the star, particularly in massive white dwarfs, the values of the pulsation periods are thus expected to be affected when sedimentation of ^{22}Ne is allowed to operate. This is demonstrated in Figures 5 and 6 for the same

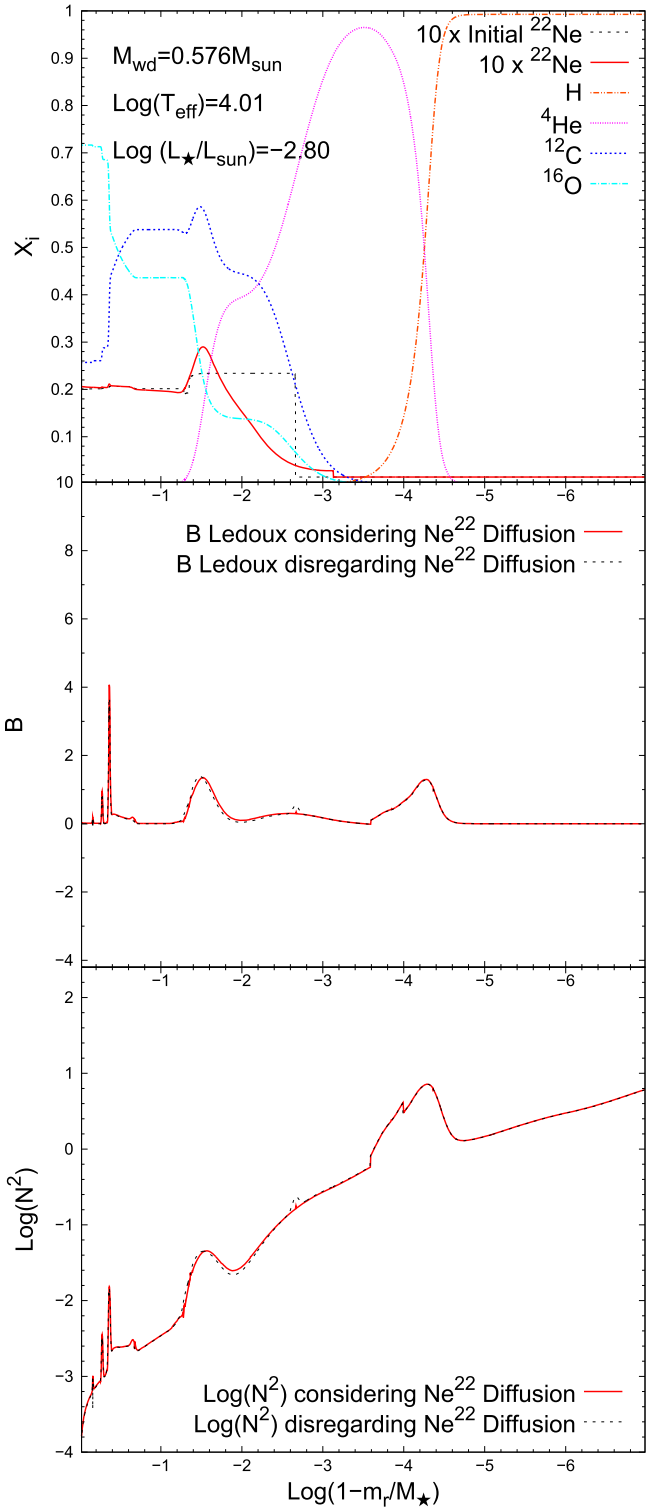

Figure 3. Top panel: chemical abundance distribution of a selected 0.576 $M_{\odot}$ white dwarf model at $\log(T_{\rm eff}) = 4.01$. For comparison purposes, the initial ^{22}Ne distribution at the beginning of the cooling track is also shown. Middle panel: Ledoux term for the same model. The solid red line corresponds to the case when ^{22}Ne sedimentation is included; the dotted line corresponds to the case when ^{22}Ne sedimentation is disregarded. Bottom panel: run of the corresponding Brunt–Väisälä frequency.

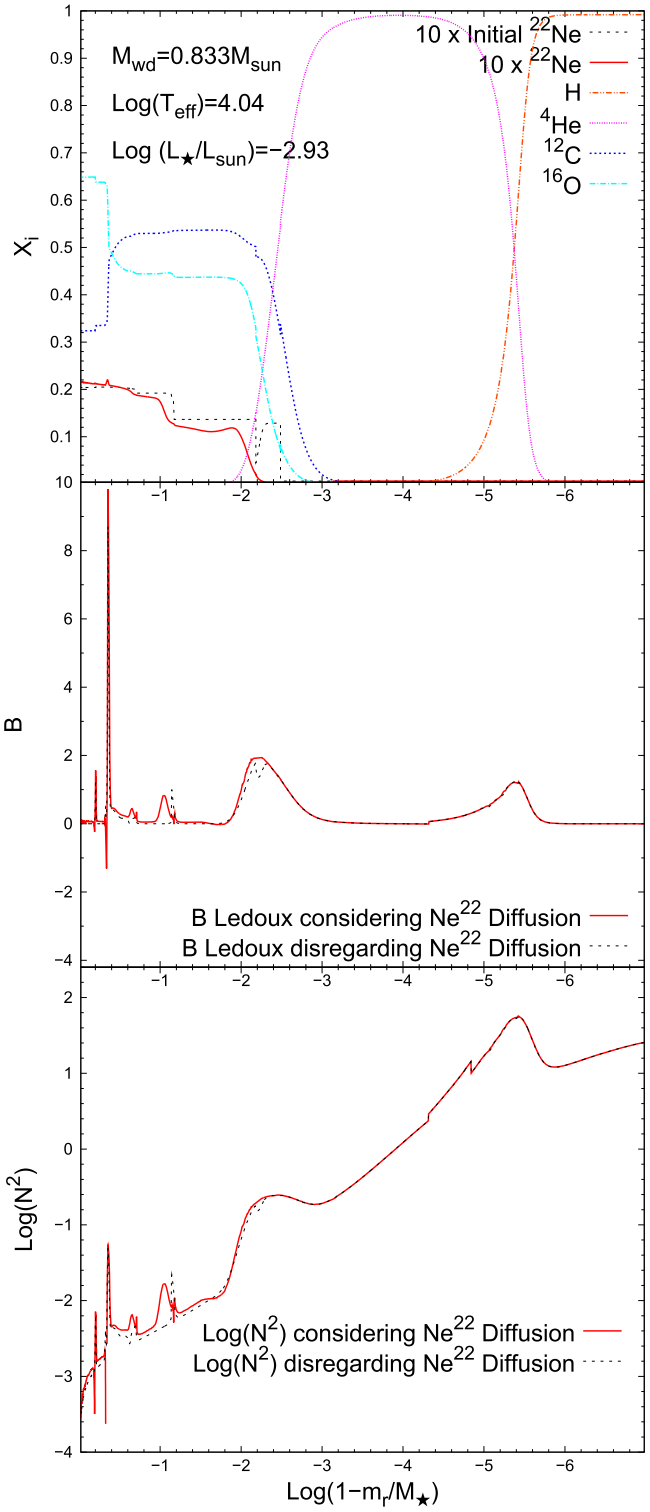

Figure 4. Same as Figure 3, but for a 0.833 $M_{\odot}$ white dwarf model at $\log(T_{\rm eff}) = 4.04$.

models analyzed in the previous paragraph. The upper panel of each figure shows the $\ell = 1$ pulsation periods, Π, as a function of the radial order k. The middle and bottom panels illustrate, respectively, the difference in the periods induced by the sedimentation process of ^{22}Ne, $\Pi_k^{\rm ND} - \Pi_k^{\rm D}$, and the forward period spacing, $\Delta\Pi_k$ ($\equiv \Pi_{k+1} - \Pi_k$). The squared symbols (in red) correspond to the case when ^{22}Ne sedimentation is considered and the cross symbols (in black) for the case in which diffusion is disregarded. In the case of the low-mass white dwarf model, the impact of ^{22}Ne sedimentation on the

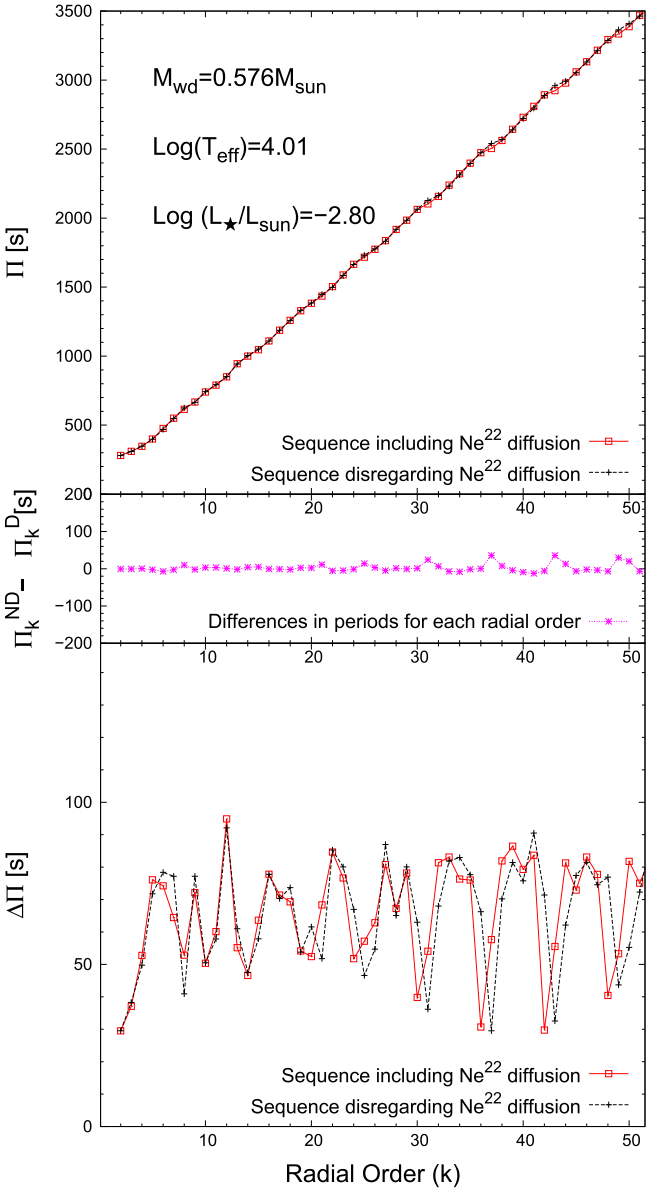

Figure 5. Top, middle, and bottom panel show, respectively, the pulsation periods in terms of the radial order k, the difference in the periods induced by ^{22}Ne sedimentation for each radial order, and the forward period spacing. The square symbols correspond to the case in which ^{22}Ne diffusion process is included; the cross symbols correspond to the case in which ^{22}Ne diffusion process is disregarded. Quantities are for a 0.576 $M_{\odot}$ white dwarf model at $\log(T_{\rm eff}) = 4.01$.

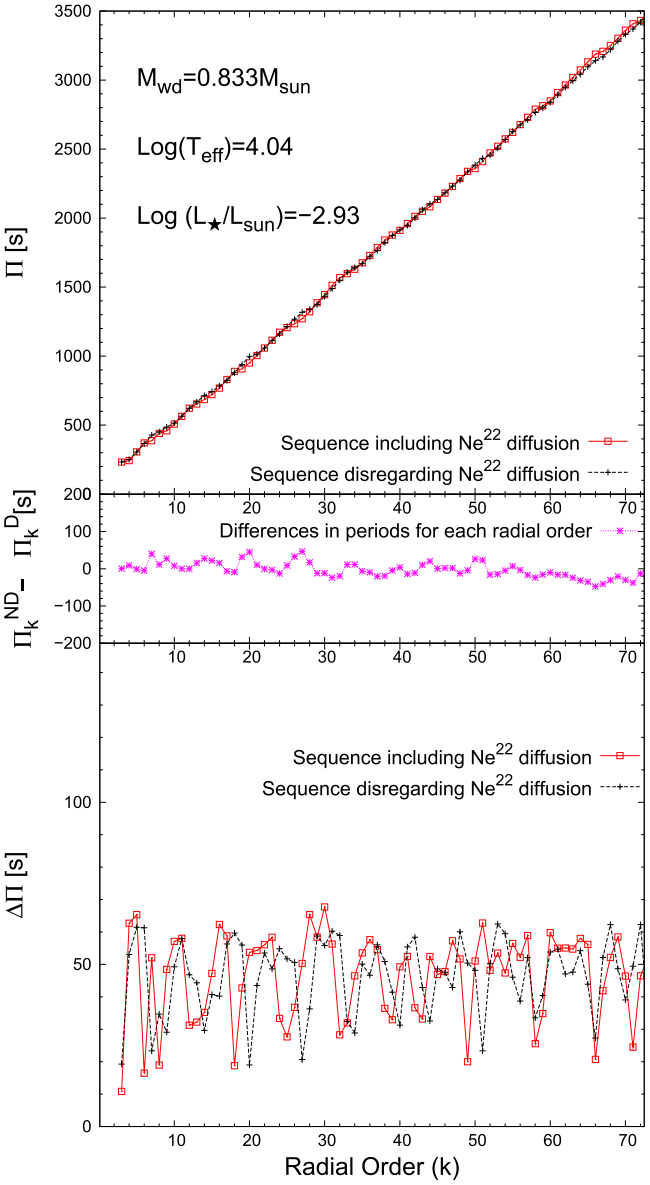

Figure 6. Same as Figure 5, but for a 0.833 $M_{\odot}$ white dwarf at $\log(T_{\rm eff}) = 4.04$.

pulsation periods is small and barely appreciable in the plot. The period differences, $|\Pi_k^{\rm ND} - \Pi_k^{\rm D}|$, between the models with and without ^{22}Ne sedimentation in the range of the periods observed in ZZ Ceti stars (from 100 to 1500 s) are on average ∼3 s, reaching values as high as ∼11 s. Although these differences are not large, they are still comparable to the typical average residual in model fits to the observed periods of pulsating white dwarfs (1–3 s) Finally, the forward period spacing (which is extremely sensitive to the precise shape of the chemical profiles) also experiences a noticeable change when we take into account ^{22}Ne sedimentation, as it is displayed in the bottom panel of this figure. In summary, the effects of ^{22}Ne sedimentation on the pulsational properties of our model are appreciable for modes with very long periods (high radial orders). However, we do not expect a large impact on the g-mode period spectrum of average-mass ZZ Ceti stars in the range of periods typically observed in these pulsating white dwarfs.

The situation is quite different for the case of more massive white dwarfs, where ^{22}Ne sedimentation becomes much more relevant. This can be deduced from Figure 6 for a selected white dwarf model of our most massive sequence. Now the differences in the theoretical periods that result from including ^{22}Ne sedimentation are on average ∼15 s, with values as high as ∼47 s. These differences are by far much larger than the typical average residual in model fits to the observed periods of pulsating white dwarfs. The impact of considering ^{22}Ne sedimentation on the forward period spacing is also noteworthy for this massive white dwarf model. Note that the effects are larger for higher radial orders (long periods). Although our results show that ^{22}Ne sedimentation affects the pulsation periods, it could still be difficult to infer its presence from a

particular signature in the pulsation spectrum, as these differences may be mimicked by other changes in the models.

The rate of period change, $d\Pi/dt$, which depends on the chemical composition of the core, is also affected by ^{22}Ne sedimentation. This quantity is related to the rate of change in the temperature of the isothermal core ($\dot{T}$) through the equation

$$\frac{\dot{P}}{P} = -a\frac{\dot{T}}{T} + b\frac{\dot{R}_\star}{R_\star}, \quad (5)$$

where a and b are dimensionless constants of the order of unity depending on the equation of state, the thicknesses of the hydrogen and helium layers, the chemical composition, among others parameters (Winget et al. 1983). Usually, for white dwarfs with hydrogen-rich atmospheres in the ZZ Ceti instability strip, the second term of the right-hand side of Equation (5) is negligible. The impact of considering ^{22}Ne sedimentation on the rates of period change at $\log(T_{\rm eff}) \sim 4$ is larger for the more massive white dwarf model (0.833 $M_\odot$) than for the 0.576 $M_\odot$ model. In the case of the more massive white dwarf model with $\log(T_{\rm eff}) = 4.04$, the temporal rates of period change obtained by the calculations are on average $\sim 3 \times 10^{-15}$ s/s larger for the sequences that neglect ^{22}Ne diffusion. This result was somehow expected, as these sequences cool faster than the ones that include ^{22}Ne diffusion. In the case of the 0.576 $M_\odot$ white dwarf model with $\log(T_{\rm eff}) = 4.01$, no appreciable difference on average in the temporal rates of period change induced by ^{22}Ne diffusion was obtained. At this point in the evolution ($\log(L/L_\odot) = -2.8$), the rate of change in the temperature of the isothermal core is still not affected by the ^{22}Ne sedimentation process (see 2). Thus, no difference in $d\Pi/dt$ is expected to occur as a consequence of this process.

4. SUMMARY AND CONCLUSIONS

The sedimentation of ^{22}Ne is a well-established physical process that has been shown to be an important source of gravitational energy during the cooling of white dwarfs descending from metal-rich progenitor stars (Deloye & Bildsten 2002; García-Berro et al. 2008; Althaus et al. 2010c). The reason behind this is that the neutron excess that characterizes the ^{22}Ne nucleus yields a net downward force and, consequently, in the liquid regions of the star ^{22}Ne slowly diffuses toward the center of the white dwarf (Bravo et al. 1992).

Observational evidence for the occurrence of ^{22}Ne sedimentation in the liquid interior of white dwarfs has been provided by García-Berro et al. (2010). However, most of the existing cooling sequences do not take this process into account. The only exceptions are the works of García-Berro et al. (2008) and Althaus et al. (2010c), who calculated grids of evolutionary cooling sequences of white dwarfs descended from metal-rich progenitors, hence with high ^{22}Ne abundances. In summary, a realistic assessment of the delay caused by ^{22}Ne sedimentation in the cooling of white dwarfs resulting from solar metallicity progenitors was lacking. Although the role of ^{22}Ne sedimentation becomes less relevant when the metal content of white dwarf progenitors is smaller, the effect of ^{22}Ne diffusion on the cooling of white dwarfs with solar metallicity might not be entirely negligible (Althaus et al. 2010c). In this context, the aim of this paper was to provide a grid of cooling sequences for such white dwarfs incorporating for the first time the effect of ^{22}Ne sedimentation. To this end, we computed the full evolution of 0.528, 0.576, 0.657, and 0.833 $M_\odot$ white dwarf models resulting from the complete evolution of progenitor stars of 1.0, 1.5, 3.0, and 4.0 $M_\odot$ from the ZAMS all the way through the phases of hydrogen and helium core burning to the thermally pulsing AGB phase. In this way, our white dwarf cooling sequences incorporate realistic initial ^{22}Ne profiles as dictated by nuclear burning history of the progenitor star. In addition, we computed ^{22}Ne sedimentation using the most recent and reliable ^{22}Ne diffusion coefficients (Hughto et al. 2010). Our computations also take into account all of the relevant energy sources, including latent heat and phase separation during crystallization.

We found that ^{22}Ne sedimentation leads to a substantial lengthening of the evolutionary times at low luminosities of white dwarfs resulting from solar metallicity progenitors. In particular, at $\log(L/L_\odot) \approx -4.5$, time delays range from 0.7 to 1.2 Gyr, depending on the stellar mass. These delays in the cooling times are not negligible whatsoever. In fact, they are much longer than the uncertainties in white dwarf cooling times due to current uncertainties in the stellar microphysics.

We extend the scope of the paper by investigating the impact of ^{22}Ne sedimentation on the adiabatic pulsational properties of ZZ Ceti models. To this end, we performed a pulsation analysis of nonradial g-modes. By the time evolution has proceeded to the ZZ Ceti domain, element diffusion has notably altered the ^{22}Ne distribution in the inner regions of the star. This has consequences for the Brunt–Väisälä frequency. In particular, for low-mass ZZ Ceti models we find that the period differences in the range of the periods observed in ZZ Ceti stars (100–1500 s) are up to ~11 s. The rate of period change in low-mass ZZ Ceti models are not affected by ^{22}Ne sedimentation process. The situation is different in the case of more massive stars, for which ^{22}Ne sedimentation becomes much more relevant. Here, we find that differences in the theoretical periods that result from including ^{22}Ne sedimentation reach values as high as ~47 s. The forward period spacings and the rate of period change are also affected.

We conclude that ^{22}Ne sedimentation is a relevant source of energy for white dwarfs resulting from solar metallicity progenitors that should be taken into account in the computation of realistic cooling sequences for these stars, as well as in attempts to perform precise asteroseismology of ZZ Ceti stars. In particular, in the light of our findings, ^{22}Ne sedimentation induces non-negligible changes in the pulsation periods and the period spacings of ZZ Ceti stars. Therefore, new asteroseismological analysis of ZZ Ceti stars should be done using stellar models that include ^{22}Ne sedimentation. In particular, a reanalysis on G117−B15A—the most well-studied ZZ Ceti star—could help to find out whether its main period (at ~215 s), for which it has been possible to measure the secular rate of change, is indeed a mode trapped in the stellar envelope or not. This is a crucial aspect in the context of the derivation of the mass of the axion from pulsating white dwarfs Isern et al. (2010), Córsico et al. (2012).

We acknowledge the valuable comments of our referee that improved the original version of this paper. Part of this work was supported by AGENCIA through the Programa de Modernización Tecnológica BID 1728/OC-AR; by the PIP 112-200801-00940 grant from CONICET; by MINECO grants

AYA2014-59084-P and ESP2014-56003-R; by the European Union FEDER funds; and by grants 2014SGR-1458 and 2014SGR-0038 (Generalitat of Catalunya). This research has made use of NASA Astrophysics Data System.

REFERENCES

Althaus, L. G., Camisassa, M. E., Miller Bertolami, M. M., Córsico, A. H., & García-Berro, E. 2015, A&A, 576, A9
Althaus, L. G., Córsico, A. H., Bischoff-Kim, A., et al. 2010a, ApJ, 717, 897
Althaus, L. G., Córsico, A. H., Isern, J., & García-Berro, E. 2010b, A&ARv, 18, 471
Althaus, L. G., García-Berro, E., Isern, J., & Córsico, A. H. 2005, A&A, 441, 689
Althaus, L. G., García-Berro, E., Isern, J., Córsico, A. H., & Miller Bertolami, M. M. 2012, A&A, 537, A33
Althaus, L. G., García-Berro, E., Renedo, I., et al. 2010c, ApJ, 719, 612
Althaus, L. G., Miller Bertolami, M. M., & Córsico, A. H. 2013, A&A, 557, A19
Bono, G., Salaris, M., & Gilmozzi, R. 2013, A&A, 549, A102
Bravo, E., Isern, J., Canal, R., & Labay, J. 1992, A&A, 257, 534
Cassisi, S., Potekhin, A. Y., Pietrinferni, A., Catelan, M., & Salaris, M. 2007, ApJ, 661, 1094
Córsico, A. H., & Althaus, L. G. 2006, A&A, 454, 863
Córsico, A. H., Althaus, L. G., Miller Bertolami, M. M., et al. 2012, MNRAS, 424, 2792
Deloye, C. J., & Bildsten, L. 2002, ApJ, 580, 1077
Dziembowski, W. A. 1971, AcA, 21, 289
Ferguson, J. W., Alexander, D. R., Allard, F., et al. 2005, ApJ, 623, 585
Fontaine, G., & Brassard, P. 2008, PASP, 120, 1043
Freytag, B., Ludwig, H.-G., & Steffen, M. 1996, A&A, 313, 497
García-Berro, E., Althaus, L. G., Córsico, A. H., & Isern, J. 2008, ApJ, 677, 473
García-Berro, E., Torres, S., Althaus, L. G., et al. 2010, Natur, 465, 194
Hansen, B. M. S., Kalirai, J. S., Anderson, J., et al. 2013, Natur, 500, 51
Herwig, F., Bloecker, T., Schoenberner, D., & El Eid, M. 1997, A&A, 324, L81
Horowitz, C. J., Schneider, A. S., & Berry, D. K. 2010, PhRvL, 104, 231101
Hughto, J., Schneider, A. S., Horowitz, C. J., & Berry, D. K. 2010, PhRvE, 82, 066401
Iglesias, C. A., & Rogers, F. J. 1996, ApJ, 464, 943
Isern, J., García-Berro, E., Althaus, L. G., & Córsico, A. H. 2010, A&A, 512, A86
Isern, J., Hernanz, M., Mochkovitch, R., & Garcia-Berro, E. 1991, A&A, 241, L29
Jeffery, E. J., von Hippel, T., DeGennaro, S., et al. 2011, ApJ, 730, 35
Miller Bertolami, M. M. 2015, arXiv:1512.04129
Miller Bertolami, M. M., Althaus, L. G., Unglaub, K., & Weiss, A. 2008, A&A, 491, 253
Miller Bertolami, M. M., Rohrmann, R. D., Granada, A., & Althaus, L. G. 2011, ApJL, 743, L33
Renedo, I., Althaus, L. G., Miller Bertolami, M. M., et al. 2010, ApJ, 717, 183
Rohrmann, R. D., Althaus, L. G., García-Berro, E., Córsico, A. H., & Miller Bertolami, M. M. 2012, A&A, 546, A119
Salaris, M., Althaus, L. G., & García-Berro, E. 2013, A&A, 555, A96
Salaris, M., Cassisi, S., Pietrinferni, A., Kowalski, P. M., & Isern, J. 2010, ApJ, 716, 1241
Tassoul, M., Fontaine, G., & Winget, D. E. 1990, ApJS, 72, 335
Torres, S., García-Berro, E., Althaus, L. G., & Camisassa, M. E. 2015, A&A, 581, A90
Unno, W., Osaki, Y., Ando, H., Saio, H., & Shibahashi, H. 1989, in Nonradial Oscillations of Stars (2nd ed.; Tokyo: Univ. Tokyo Press), 160
Wachlin, F. C., Miller Bertolami, M. M., & Althaus, L. G. 2011, A&A, 533, A139
Weiss, A., & Ferguson, J. W. 2009, A&A, 508, 1343
Winget, D. E., Hansen, C. J., & van Horn, H. M. 1983, Natur, 303, 781
Winget, D. E., & Kepler, S. O. 2008, ARA&A, 46, 157
Winget, D. E., Kepler, S. O., Campos, F., et al. 2009, ApJL, 693, L6